# Nonlinear Hydrostatic Adjustment

PETER R. BANNON

*Department of Meteorology, The Pennsylvania State University, University Park, Pennsylvania*

(Manuscript received 6 September 1995, in final form 18 June 1996)

ABSTRACT

The final equilibrium state of Lamb's hydrostatic adjustment problem is found for finite amplitude heating. Lamb's problem consists of the response of a compressible atmosphere to an instantaneous, horizontally homogeneous heating. Results are presented for both isothermal and nonisothermal atmospheres.

As in the linear problem, the fluid displacements are confined to the heated layer and to the region aloft with no displacement of the fluid below the heating. The region above the heating is displaced uniformly upward for heating and downward for cooling. The amplitudes of the displacements are larger for cooling than for warming.

Examination of the energetics reveals that the fraction of the heat deposited into the acoustic modes increases linearly with the amplitude of the heating. This fraction is typically small (e.g., 0.06% for a uniform warming of 1 K) and is essentially independent of the lapse rate of the base-state atmosphere. In contrast a fixed fraction of the available energy generated by the heating goes into the acoustic modes. This fraction (e.g., 12% for a standard tropospheric lapse rate) agrees with the linear result and increases with increasing stability of the base-state atmosphere.

The compressible results are compared to solutions using various forms of the soundproof equations. None of the soundproof equations predict the finite amplitude solutions accurately. However, in the small amplitude limit, only the equations for deep convection advanced by Dutton and Fichtl predict the thermodynamic state variables accurately for a nonisothermal base-state atmosphere.

## 1. Introduction

Lamb's problem (Bannon 1995a) has been advanced as the prototype example of hydrostatic adjustment by acoustic modes. This problem consists of the response of a stably stratified atmosphere to an instantaneous heating that is vertically confined but horizontally uniform. Solutions of this problem have addressed the transient evolution of the flow, the final equilibrium state, and its energetics in the context of linear dynamics for an isothermal atmosphere.

The purpose of the present investigation is to solve for the final equilibrium in Lamb's problem in a nonlinear context for an atmosphere of arbitrary thermal structure. These solutions address several issues. One result of the linear problem is that there is no displacement of the fluid below the heating while there is a uniform displacement above the heating. The nonlinear solutions presented demonstrate the robustness of this finding. A second motivation focuses on the energetics. Nicholls and Pielke (1994) have noted the disparity in the formulation of the energetics of the linear and the nonlinear problems. This disparity is removed here by using the generalized theory of Andrews (1981) for available potential energy.

The nonlinear solution will also be used to distinguish between heating and cooling. In the linear problem, the solutions for cooling are those for heating with a change in sign. Thus, for example, the fluid above the cooled layer sinks rather than rises as a result of the contraction of the cooled layer rather than the expansion of the warmed layer. However, the linear energetics are quadratic in the perturbations and are identical for heating and cooling. The nonlinear problem breaks this symmetry and differentiates between the two cases.

Lastly, the previous results (Bannon 1995a) are extended to a base-state atmosphere of arbitrary thermal structure. This extension enables one to discriminate among the anelastic theories of Dutton and Fichtl (1969), Miller (1974), and Lipps and Hemler (1982) that incorporate the adjustment process equally well for an isothermal atmosphere.

Section 2 describes the nonlinear problem and its solution. The Lagrangian method of solution finds an equation for the vertical displacement of the fluid parcels. The approach is the analog to the nonlinear treatment of the Rossby (Mihaljan 1963) and the Gill (Glendening 1993) adjustment problem. The closed form expression for the vertical displacement is evaluated analytically for small amplitude heating and numerically for finite amplitude heating. Section 3 con-

*Corresponding author address:* Dr. Peter R. Bannon, Department of Meteorology, The Pennsylvania State University, 503 Walker Building, University Park, PA 16802-5013.
E-mail: bannon@ems.psu.edu

siders the energetics using the traditional approach in terms of internal and potential energy while section 4 presents the energetics in terms of available energy. Section 5 examines the ability of various versions of the soundproof equations to incorporate the adjustment. Section 6 briefly summarizes the major results.

## 2. Nonlinear problem and its solution

### a. Model formulation

The model atmosphere is a horizontally homogeneous, inviscid, compressible fluid in a Cartesian coordinate system where $-g\mathbf{k}$ is the acceleration due to gravity. The atmosphere is completely described by the Lagrangian quantities,

$$z, p, T, \rho, \quad \text{and} \quad \theta, \tag{2.1}$$

denoting the vertical position, pressure, temperature, density, and potential temperature of a fluid parcel, respectively. The base state of the stably stratified atmosphere before the heating is denoted with the subscript naught. Then $z = z(z_0, t)$ describes the vertical position of the fluid parcel originally at $z_0$ as it varies with time $t$. The base-state temperature, $T_0 = T(z_0, t = 0)$, is a prescribed function of height, and the other state variables satisfy

$$\frac{dp_0}{dz_0} = -\rho_0 g, \quad \theta_0 = T_0\left(\frac{p_*}{p_0}\right)^{R/C_p},$$

$$p_0 = \rho_0 R T_0, \tag{2.2}$$

where $R$ is the ideal gas constant and $C_p$ is the specific heat at constant pressure. The values of the base-state variables at $z = 0$ are denoted with an asterisk subscript, for example,

$$p_* \equiv p_0\,(z = 0), \tag{2.3}$$

and are constants.

At the time $t = 0$, say, the atmosphere is subjected to an instantaneous heating rate per unit volume of the form

$$Q = Q_{00} q(z)\delta(t), \tag{2.4}$$

where $Q_{00}$ is the constant amplitude of the energy per unit volume (positive for heat added; negative for heat extracted) and $\delta$ is the Dirac delta function. Here $q(z)$ describes the vertical distribution of the heating with the origin $z = 0$ taken to be the center of the heating. The atmosphere is semi-infinite with a flat rigid lower boundary at $z = -b$.

We define the initial state as that of the atmosphere immediately after the heating has occurred but before there has been any motion. Mathematically, the initial state is given by the quantities in (2.1) with a subscript $i$. For example, $z_i = z(z_0, t = 0^+)$ is the position of the fluid parcel originally at $z_0$. The initial state is related to the base state by

$$z_i = z_0, \tag{2.5a}$$

$$\rho_i = \rho_0, \tag{2.5b}$$

$$T_i = T_0 + \delta T, \tag{2.5c}$$

$$p_i = \rho_i R T_i, \tag{2.5d}$$

$$\theta_i = T_i\left(\frac{p_*}{p_i}\right)^{R/C_p}, \tag{2.5e}$$

where

$$\delta T = \frac{Q_{00} q(z_0)}{\rho_0 C_v}. \tag{2.6}$$

The heat exchange occurs at constant volume and produces a change in temperature, pressure, and potential temperature, while leaving the density unaltered. This process generates a hydrostatic imbalance since the pressure is altered but not the density.

### b. Exact solution for the final equilibrium

Conservation of mass and entropy enables the determination of the final equilibrium state. This hydrostatic equilibrium is denoted with the subscript $f$. For example, $z_f = z(z_0, t = \infty)$ is the final position of the fluid parcel originally at $z_0$. Mass conservation may be written as

$$\rho_f dz_f = \rho_i dz_i = \rho_0 dz_0. \tag{2.7}$$

Then the mass of air above a fluid parcel remains unchanged. Since both the final and base states are in hydrostatic balance,

$$dp_0 = -\rho_0 g dz_0 \quad dp_f = -\rho_f g dz_f, \tag{2.8}$$

(2.7) implies that the final pressure of a parcel is its value originally:

$$p_f = p_0. \tag{2.9}$$

The statement of the conservation of entropy is

$$\theta_f = \theta_i. \tag{2.10}$$

From Poisson's relation, the final density field is

$$\rho_f = \frac{p_*^{R/C_p}}{R}\frac{p_f^{1/\gamma}}{\theta_f} = \frac{p_*^{R/C_p}}{R}\frac{p_0^{1/\gamma}}{\theta_i}, \tag{2.11}$$

where $\gamma = C_p/C_v$ and $C_v = C_p - R$. The second equality is a consequence of (2.9) and (2.10). From the ideal gas law, the final temperature field is given by

$$T_f = \frac{p_f}{\rho_f R} = \frac{p_0}{\rho_f R}. \tag{2.12}$$

Specification of (2.1) for the final state is completed with an expression for the final parcel position $z_f$. From mass conservation (2.7),

$$dz_f = \frac{\rho_i}{\rho_f} dz_i = \frac{\rho_0}{\rho_f} dz_0. \tag{2.13}$$

Use of Poisson's relation and (2.9) yields

$$dz_f = \frac{\theta_i}{\theta_0} dz_0. \tag{2.14}$$

Integration upward from the flat rigid lower boundary at $z = -b$ yields

$$z_f(z_0) = -b + \int_{-b}^{z_0} \frac{\theta_i(z)}{\theta_0(z)} dz, \tag{2.15}$$

where $z$ has been introduced as the dummy variable of integration. The vertical displacement $\zeta$ of a fluid parcel is

$$\zeta(z_0) \equiv z_f - z_i = \int_{-b}^{z_0} \left[ \frac{\theta_i(z)}{\theta_0(z)} - 1 \right] dz. \tag{2.16}$$

A useful alternative expression for (2.16) is, using (2.5) and (2.6),

$$\zeta(z_0) = \int_{-b}^{z_0} \left\{ \left[ 1 + \frac{Q_{00} q(z)}{\rho_0 C_v T_0} \right]^{1/\gamma} - 1 \right\} dz. \tag{2.17}$$

Inspection of (2.16) indicates that the relative displacement is zero for all parcels below the heating, while $\zeta$ is a constant above the heating. Thus, as in the linear problem, the fluid expands upward and the fluid below the heating remains unaltered by the adjustment. Similarly, the fluid above the heating is unaltered apart from a finite vertical displacement. The expansion of the heated layer reduces the density and cools the layer adiabatically to produce a continuous pressure field in hydrostatic balance.

Figure 1 provides a schematic of the adjustment of the thermodynamic state variables. In order to visualize the adjustment better, the schematic is drawn for the case of a top hat heating profile. The parcels above the heated region are lifted uniformly upward with no change in their state variables. The heated region responds by expanding upward with a concomitant decrease in density and temperature. The fluid below the region of heating is unchanged. The choice of a top hat heating profile produces discontinuities in the potential temperature field at the top and bottom of the layer of heated fluid. The upper discontinuity is statically unstable. This shortcoming is overcome with more smoothly varying heating profiles.

Thermodynamically, the hydrostatic adjustment problem is a two-step process. Starting from the base state, an air parcel is heated at constant volume, thereby increasing its pressure, temperature, and entropy. The heated parcel then expands and cools adiabatically back to its base-state pressure. This sequence is similar to a portion of an Otto cycle (e.g., see Doolittle and Hale 1983).

It is worth noting that the present derivation is consistent with the conservation of the one-dimensional analog of potential vorticity (Bannon 1995a). Mass conservation,

$$\rho_f dz_f = \rho_i dz_i, \tag{2.18a}$$

and entropy conservation,

$$d\theta_f = d\theta_i, \tag{2.18b}$$

imply the conservation of the specific static stability:

$$\frac{d\theta_f}{\rho_f dz_f} = \frac{d\theta_i}{\rho_i dz_i}. \tag{2.19}$$

Thus, potential vorticity is conserved. It should be noted that while the solution of the linear problem explicitly uses the conservation of potential vorticity, the solution of the nonlinear problem does not. This feature appears in the nonlinear geostrophic adjustment problem of Mihaljan (1963) but not in that of Glendening (1993).

### c. *Analytic solution in the small amplitude limit*

If the heating is small, then the displacement (2.17) can be approximated as

$$\zeta(z_0) = \int_{-b}^{z_0} \frac{Q_{00} q(z)}{\rho_0 C_p T_0} dz. \tag{2.20}$$

Analytic solutions of this expression are possible for various base states and heating profiles. We consider the three heating profiles

$$q(z) = H(a^2 - z^2), \tag{2.21a}$$

$$q(z) = \frac{3}{2}\left(1 - \frac{z^2}{a^2}\right) H(a^2 - z^2), \tag{2.21b}$$

$$q(z) = \pi \sin\left(\frac{\pi z}{a}\right) H(a^2 - z^2), \tag{2.21c}$$

where $H$ is the Heaviside step function and the heating for each profile vanishes for $|z| > a$. We refer to the profiles (2.21) as the top hat, parabolic, and sinusoidal profile, respectively. Note that the top hat and parabolic profiles are normalized to have the same net heating over the region $|z| < a$. The sinusoidal heating has a mean over the region $0 < z < a$ equal to twice that of the top hat, but its net heating vanishes by symmetry over the domain $|z| < a$.

Two convenient base states are an isothermal atmosphere with

$$T_0 = T_*, \quad \rho_0 = \rho_* e^{-z/H_S}, \quad H_S = RT_*/g, \tag{2.22a}$$

and an atmosphere with a constant lapse rate $\Gamma$:

$$T_0 = T_* - \Gamma z, \quad \rho_0 = \rho_* \left(\frac{T}{T_*}\right)^{(g/\Gamma R - 1)}. \tag{2.22b}$$

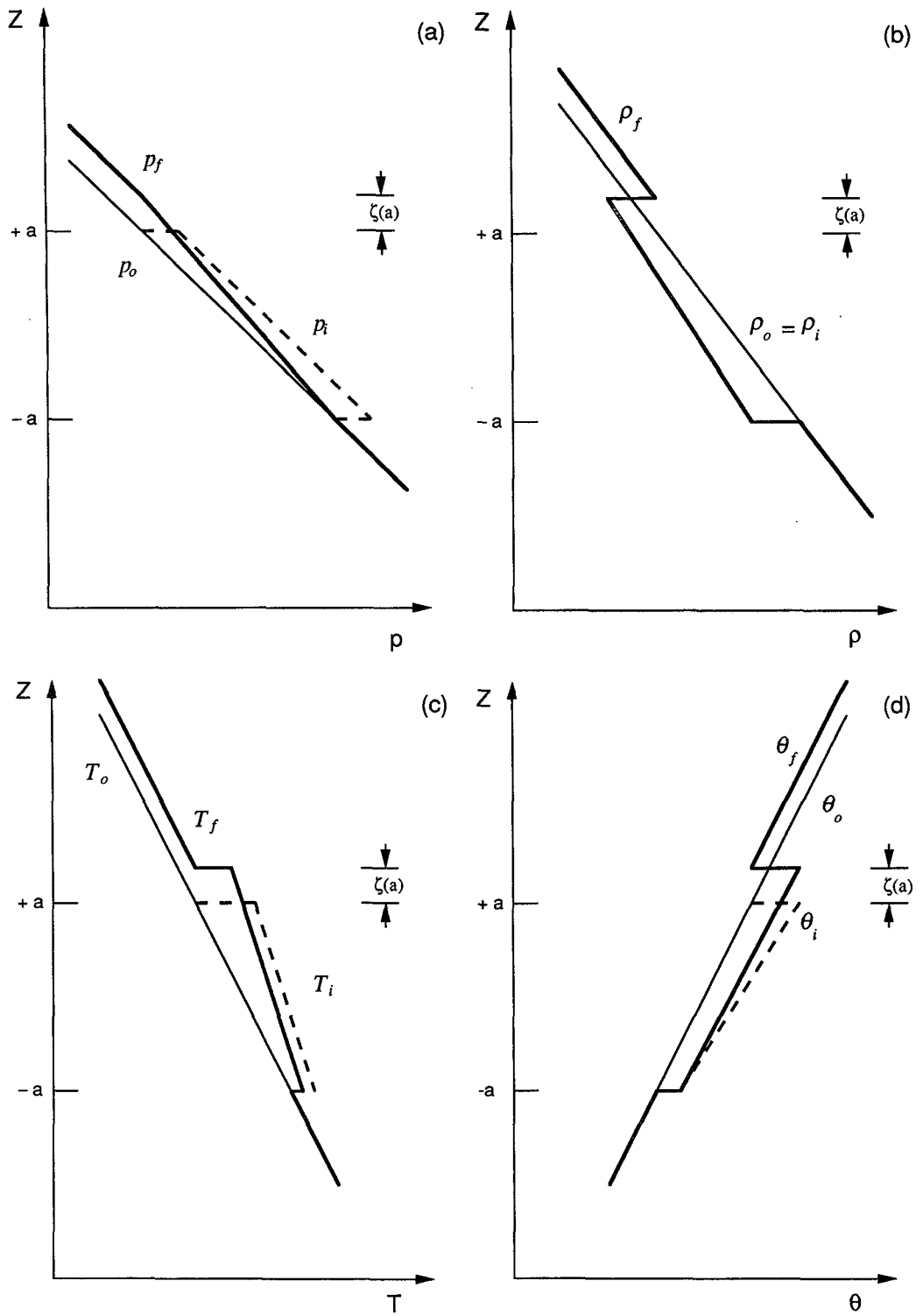


FIG. 1. Schematic illustration of the hydrostatic adjustment of a layer of width $2a$ heated uniformly. Panels (a), (b), (c), and (d) refer to the pressure, density, temperature, and potential temperature fields, respectively. The thin solid line denotes the base-state atmosphere, the dash line the initial field immediately after the heating, and the heavy solid line the final equilibrium.

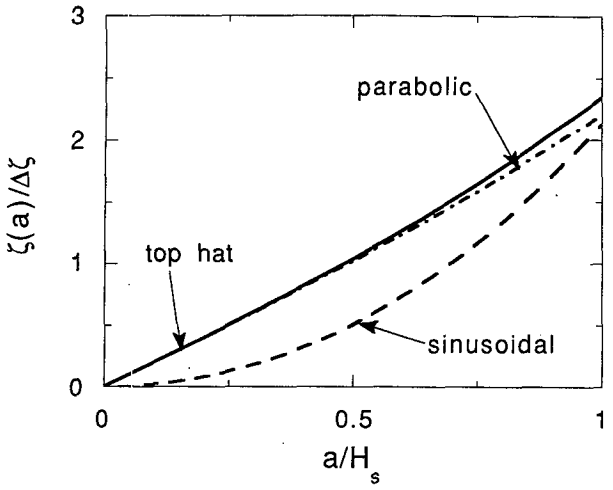


FIG. 2. Vertical displacement at the top of the heated layer as a function of heating half width $a$ in the linear case for various heating profiles for an isothermal atmosphere.

The asterisk subscript again denotes a variable's reference value at $z = 0$.

The solutions for the displacement at the top of the heating for an isothermal atmosphere are

$$\zeta(a) = 2\Delta\zeta \sinh\left(\frac{a}{H_S}\right), \tag{2.23a}$$

$$\zeta(a) = 6\Delta\zeta\left[\frac{H_S}{a}\cosh\left(\frac{a}{H_S}\right) - \left(\frac{H_S}{a}\right)^2 \sinh\left(\frac{a}{H_S}\right)\right], \tag{2.23b}$$

$$\zeta(a) = 2\Delta\zeta\frac{\left(\frac{a}{H_S}\right)\sinh\left(\frac{a}{H_S}\right)}{\left(1 + \frac{a^2}{\pi^2 H_S^2}\right)}, \tag{2.23c}$$

for the top hat, parabolic, and sinusoidal profiles, respectively, where

$$\Delta\zeta = \frac{Q_{00}}{\rho_* C_p T_*} \quad H_S = \frac{R\Delta T}{\gamma g}. \tag{2.24}$$

Here, $Q_{00} = \rho_* C_v \Delta T$ and $\Delta T$ is the temperature change at the center of the layer.

The displacement at the top of the heated layer is plotted in Fig. 2 as a function of the heating half width $a$. The top hat result agrees with Bannon (1995a). The parabolic result is consistent with that for the top hat, but the continuous parabolic profile generates no statically unstable profiles as does that for the top hat. The sinusoidal result exhibits a nonzero displacement of the top of the heated layer despite the fact that the net heating for the profile is zero. A positive displacement occurs because warming occurs aloft in the less dense air where the accelerations are larger (Bannon 1995a). For heating of small vertical extent this effect is negligible and $\zeta(a) \sim 2\Delta\zeta(a/H_S)^2 \sim 0$.

For an atmosphere with a constant lapse rate $\Gamma$, the displacement at the top of the heated layer for a top hat heating profile is

$$\zeta(a) = \frac{\Delta\zeta}{\left(1 - \frac{\Gamma}{\Gamma_a}\right)}\left[\frac{T_0^c(+a) - T_0^c(-a)}{T_0^c(0)}\right], \tag{2.25}$$

where $c = 1 - \Gamma_a/\Gamma$ and $\Gamma_a = g/R$ is the autoconvective lapse rate. Evaluation of (2.25) with $a/Hs = 1/2$ yields total normalized displacements $\hat{\zeta}$,

$$\hat{\zeta} = \frac{\zeta(a)}{\Delta\zeta}, \tag{2.26}$$

of 1.0385, 1.0422, 1.0509, and 1.0556 for $\Gamma = -2.8$, 0, 6.5, and 9.8 K km$^{-1}$, respectively. Thus, the total displacement is relatively insensitive to the lapse rate.

### d. Numerical results

In general, the result (2.16) must be evaluated numerically. For definiteness the parameter settings are $T_* = 251.932$ K and $\rho_* = 0.6914$ kg m$^{-3}$, which correspond to the standard atmosphere at 500 mb. The physical constants are $g = 9.81$ m s$^{-2}$, $C_p = 1004$ m$^2$ s$^{-2}$ K$^{-1}$, and $\kappa = R/C_p = 2/7$. These settings are used for all finite amplitude results presented in this and subsequent sections.

Table 1 summarizes the effect of finite-amplitude heating on the displacement of the top of the heated layer for three different lapse rates. For fixed $\Gamma$, the linear result (2.25) slightly overestimates the amplitude of $\hat{\zeta}$ for warming but underestimates it for cooling. Note that the sign of the displacements are negative, indicating a contraction of the cooled layer. Table 1 also indicates that the amplitudes of the displacements decrease slightly with increasing static stability of the

TABLE 1. Normalized displacement, $\hat{\zeta}$, at the top of the heated layer as a function of the base-state atmospheric lapse rate $\Gamma$ and the magnitude of the heating, $\Delta T$. Values of $\hat{\zeta}$ for cooling are indicated in parentheses. Data are for a top hat heating profile with $a/H_S = 1/2$.

| | $\Delta T$ (K) | | | |
|---|---|---|---|---|
| Atmosphere | ~0 | 0.1 | 1.0 | 10.0 |
| Standard | 1.0509 | 1.0509 | 1.0503 | 1.0443 |
| $\Gamma$ = 6.5 K/km | | (−1.0510) | (−1.0516) | (−1.0579) |
| Isothermal | 1.0422 | 1.0421 | 1.0415 | 1.0357 |
| $\Gamma$ = 0 K/km | | (−1.0423) | (−1.0429) | (−1.0490) |
| Inversion | 1.0385 | 1.0385 | 1.0379 | 1.0321 |
| $\Gamma$ = −2.8 K/km | | (−1.0386) | (−1.0392) | (−1.0453) |

Amplitudes of the displacement, $\hat{\zeta}$, are identical for heating and cooling in the linear case ($\Delta T \sim 0$), apart from a change in sign.

base state. Results for other heating profiles are similar to those presented in Table 1 for the top hat profile and are not shown.

Table 1 suggests a power series expansion of the integrand in (2.17) would yield fairly accurate results. One finds

$$\zeta(a) = \tau \int_{-a}^{+a} \hat{q}(z)dz - \frac{(\gamma - 1)}{2}\tau^2 \times \int_{-a}^{+a} [\hat{q}(z)]^2 dz + \frac{(\gamma - 1)(2\gamma - 1)}{6}\tau^3 \times \int_{-a}^{+a} [\hat{q}(z)]^3 dz + \cdots, \quad (2.27)$$

where

$$\hat{q}(z) \equiv \frac{\rho_* T_*}{\rho_0 T_0} q(z) \quad (2.28)$$

is the nondimensional profile of the initial warming and is $O(1)$. The relevant nondimensional expansion parameter $\tau$ is

$$\tau \equiv \frac{\Delta T}{\gamma T_*}, \quad (2.29)$$

where $\Delta T$ is the initial temperature change at the center of the heating, where the base-state temperature is $T_*$. Then $\tau$ is a measure of the strength of the heating. The factor of $\gamma = C_p/C_v$ reflects the fact that the initial warming occurs at constant volume while, the final temperature change is at constant pressure [recall (2.9)]. The first term in (2.27) is the linear result (2.20). The second is the lowest order nonlinear correction. For simplicity let $\hat{q} = 1$, then

$$\frac{\zeta(a)}{\Delta\zeta} \sim 1 - \frac{\gamma - 1}{2}\tau, \quad (2.30)$$

and the difference between heating $\tau > 0$ and cooling $\tau < 0$ is $(\gamma - 1)\tau = 0.0001$, 0.001, and 0.011 for $\Delta T = 0.1$, 1.0, and 10.0 K, respectively. The results in Table 1 are well estimated by the first two terms in (2.27).

## 3. Traditional energetics

The total static energy, TE, is the sum of the internal, IE, and potential, PE, energy:

$$\text{TE} = \text{IE} + \text{PE}, \quad (3.1)$$

where

$$\text{IE} = \int_{-b}^{\infty} \rho C_v T dz, \quad (3.2)$$

$$\text{PE} = \int_{-b}^{\infty} \rho g z dz. \quad (3.3)$$

It is well known that, for a hydrostatic atmosphere,

$$\text{PE} = \frac{R}{C_v}\text{IE} \quad (3.4a)$$

and

$$\text{TE} = \gamma\text{IE} = \frac{1}{\kappa}\text{PE}, \quad (3.4b)$$

where $\gamma = C_p/C_v$ and $\kappa = R/C_p$.

As a result of the heating, the internal energy of the heated layer has increased:

$$\text{IE}_i = \text{IE}_0 + \Delta Q, \quad (3.5a)$$

where

$$\Delta Q = \int_{-b}^{\infty} \rho C_v \delta T dz,$$

while the potential energy of the fluid is initially unchanged,

$$\text{PE}_i = \text{PE}_0. \quad (3.5b)$$

During the adjustment to the final equilibrium, the potential energy increases,

$$\text{PE}_f = \text{PE}_i + \Delta\text{PE} \quad \text{where} \quad \Delta\text{PE} = \int_{-b}^{\infty} \rho g \zeta dz, \quad (3.6)$$

and the internal energy decreases,

$$\text{IE}_f = \text{IE}_i + \Delta\text{IE} \quad \text{where}$$

$$\Delta\text{IE} = \int_{-b}^{\infty} \rho C_v (T_f - T_i) dz, \quad (3.7)$$

as a result of the fluid expansion. Note that the change in internal energy is confined to the heated layer of the fluid. The change in the total static energy is

$$\Delta\text{TE} \equiv \text{TE}_i - \text{TE}_f = \text{TE}_0 + \Delta Q - \text{TE}_f = \frac{1}{\kappa}\Delta\text{PE} - \Delta Q. \quad (3.8)$$

The first equality is a consequence of (3.5); the second results from application of (3.4) to the total energy of the hydrostatic base and final states. Typically, $\Delta$TE is negative and represents the amount of wave energy, WE, lost to the acoustic modes:

$$\text{WE} = -\Delta\text{TE}. \quad (3.9)$$

Results for the finite-amplitude energetics are summarized in Fig. 3 and Table 2. Figure 3 shows that the fraction of wave energy, $E_{\text{waves}} = \text{WE}/|\Delta Q|$, is small but increases monotonically with the amplitude of the heating. To a good approximation, the slope of the curves in Fig. 3 (see also Table 2) implies

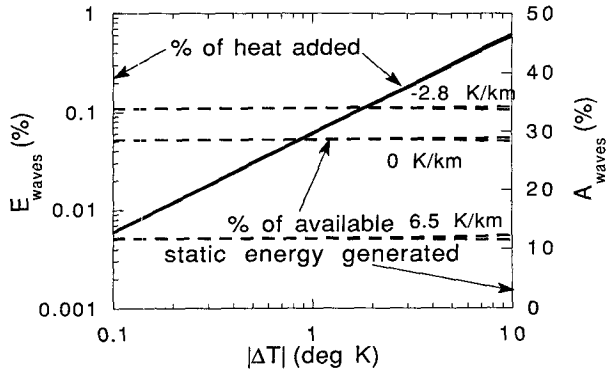


FIG. 3. Wave energy as a percent of the heat exchange, $E_{waves}$, (solid line) or as a percent of the available static energy generated, $A_{waves}$, (dash line) as a function of the heating amplitude $|\Delta T|$ for various values of the base-state lapse rate $\Gamma$ in K km$^{-1}$. Data are for a top hat heating profile with $a/H_S = 1/2$. The $E_{waves}$ curves for various $\Gamma$ and for warming and cooling overlap (see Table 2). Values of $A_{waves}$ are typically slightly larger for warming than cooling.

$$\frac{\text{WE}}{|\Delta Q|} = 6 \times 10^{-4}|\Delta T| \text{ (in K)}. \quad (3.10)$$

This result is relatively insensitive (see Table 2) to either the lapse rate of the base state or the sign of the heating.

The energy transfers differ depending on the sign of the heating. Table 2 indicates that for warming there is expansion of the heated layer with an increase in the potential energy and a decrease in the internal energy. For cooling there is a contraction of the layer with a decrease in potential energy and an increase in the internal energy. In either case the net decrease in the sum of the internal and potential energies is lost to the waves.

Table 2 also describes the partitioning of the change in potential energy between the heated layer and the fluid aloft. Most of the change occurs in the fluid aloft. This dominance increases as the extent of the heated layer decreases. For example, additional calculations find $\Delta\text{PE}_{\text{layer}} = 6.178$ and 3.315%, $\Delta\text{PE}_{\text{aloft}} = 22.378\%$ and 25.240% for a warming of $\Delta T = 1.0$ K with $a/H_S = 1/4$ and $1/8$, respectively. As noted above, the change in internal energy occurs completely in the heated layer.

It is of interest to examine the traditional energetics in the small amplitude limit. The change in potential energy [(3.6)] may be written as

$$\Delta\text{PE} = -\int_{p(-b)}^{p(\infty)} \zeta\, dp = \int_{-b}^{\infty} p\,\frac{d\zeta}{dz}\,dz, \quad (3.11)$$

where use has been made of the fact that the final state is hydrostatic. Then, integration by parts yields the final result in (3.10) after applying the boundary conditions that $\zeta(z = -b) = 0$ and $p_0(z = \infty) = 0$. Substitution of the linear result (2.20) for the relative displacement yields the general linear result

$$\Delta\text{PE}_{\text{lin}} = \kappa\Delta Q. \quad (3.12)$$

The change in PE is a fixed fraction, $\kappa$, of the heat added to the layer and equals the loss $\Delta$IE in internal energy. Thus, from (3.8), energy is conserved, $\Delta$TE = 0, and no energy is lost to the acoustic modes: WE = 0. This unphysical result indicates that it is inappropriate to apply the traditional energetics to the linear problem. The energetics of the linear problem are not governed by traditional energetics. The correct formulation of the energetics in the linear problem is given in terms of available energy, and it is meaningful to compare the linear and nonlinear energetics in this context only.

## 4. Available energetics

An alternative energy interpretation is provided in terms of available energetics (Andrews 1981). This formalism is a generalization of available potential energy for a compressible fluid. The available static energy, ASE, is the sum of the available elastic energy, AEE, and the available potential energy, APE,

$$\text{ASE} = \text{AEE} + \text{APE}. \quad (4.1)$$

The available elastic energy is defined by

$$\text{AEE} = \int_{-b}^{\infty} \rho C_p \theta \left(\frac{p_0}{p_*}\right)^{\kappa} f\left(\frac{p}{p_0}\right) dz, \quad (4.2)$$

TABLE 2. Potential and internal energy changes and wave energy normalized by the magnitude $|\Delta Q|$ of the heat exchange as a function of $\Delta T$. Units are % of $|\Delta Q|$. Potential energy change is divided into that in the heated layer and in the region aloft. Data are for a top hat heating profile with $a/H_s = 1/2$ and a lapse rate $\Gamma = 6.5$ K km$^{-1}$. Values for cooling are in parentheses.

| $\Delta T$ | $\Delta\text{PE}_{\text{layer}}$ | $\Delta\text{PE}_{\text{aloft}}$ | $\Delta$PE | $\Delta$IE | WE |
|---|---|---|---|---|---|
| 0.1 K | 10.815 | 17.755 | 28.570 | −28.576 | 0.006 |
| | (−10.816) | (−17.757) | (−28.573) | (+28.567) | (0.006) |
| 1.0 K | 10.810 | 17.745 | 28.554 | −28.614 | 0.060 |
| | (−10.821) | (−17.768) | (−28.589) | (+28.529) | (0.060) |
| 10.0 K | 10.760 | 17.644 | 28.404 | −28.989 | 0.585 |
| | (−10.872) | (−17.873) | (−28.745) | (+28.137) | (0.608) |

where

$$f(x) = (1 - \kappa)x^{\kappa} + \kappa x^{-(1-\kappa)} - 1. \quad (4.3)$$

Andrews has shown that $f(1) = 0$ and $f(x) > 0$ for $x \neq 1$. In addition the small amplitude limit of (4.2) is

$$\mathrm{AEE}_{\mathrm{lin}} = \int_{-b}^{\infty} \frac{1}{2} \frac{(p - p_0)^2}{\rho_0 c_0^2} dz, \quad (4.4)$$

with $c_0^2 = \gamma R T_0$ and agrees with linear theory (e.g., Bannon 1995a).

The available potential energy is defined as

$$\mathrm{APE} = \int_{-b}^{\infty} \rho C_p T_* h(\theta, \theta_0) dz, \quad (4.5)$$

where

$$h(\theta, \theta_0) = \frac{\theta}{\theta_0} - 1 - \ln\left(\frac{\theta}{\theta_0}\right) \quad (4.6)$$

for an isothermal atmosphere and

$$h(\theta, \theta_0) = \left(\frac{\theta - \theta_0}{\theta_*}\right)\left(\frac{\theta_0}{\theta_*}\right)^{r-1} - \frac{1}{r}\left(\frac{\theta^r - \theta_0^r}{\theta_*^r}\right) \quad (4.7)$$

for an atmosphere with a constant lapse rate $\Gamma$. Here,

$$r = \left(1 - \frac{\Gamma_d}{\Gamma}\right)^{-1} \quad \text{with} \quad \Gamma_d = g/C_p. \quad (4.8)$$

The small amplitude limit of (4.5),

$$\mathrm{APE}_{\mathrm{lin}} = \int_{-b}^{\infty} \frac{\rho_0}{2N_0^2}\left(\frac{g(\theta - \theta_0)}{\theta_0}\right)^2 dz, \quad (4.9)$$

agrees with linear theory. Andrews has shown that (4.2) and (4.5) are non-negative.

Application of this formalism to the adjustment problem is straightforward. Note that the reference state in (4.2) and (4.5) is the base-state atmosphere for which $\mathrm{ASE}_0 = \mathrm{AEE}_0 = \mathrm{APE}_0 = 0$. The heating increases the available elastic and available potential energies in the layer but not elsewhere. In the final state, $p_f = p_0$ and $\theta_f = \theta_0$ aloft so the available elastic and available potential energies vanish there. In the layer $\theta_f = \theta_i \neq \theta_0$, so the available potential energy is unaltered:

$$\Delta\mathrm{APE} = \mathrm{APE}_f - \mathrm{APE}_i = 0. \quad (4.10)$$

In contrast, there is no available elastic energy in the final state since $p_f = p_0$. The change in elastic energy,

$$\Delta\mathrm{AEE} = \mathrm{AEE}_f - \mathrm{AEE}_i = -\mathrm{AEE}_i, \quad (4.11)$$

is negative and represents the amount of available energy lost to the acoustic modes, AWE:

$$\mathrm{AWE} = -\mathrm{AEE}_i. \quad (4.12)$$

Figure 3 plots the normalized available wave energy, $A_{\mathrm{waves}}$, as a function of the amplitude of the heating. Here,

$$A_{\mathrm{waves}} \equiv \frac{\mathrm{ASE}_i - \mathrm{ASE}_f}{\mathrm{ASE}_i - \mathrm{ASE}_0} = \frac{\mathrm{AEE}_i}{\mathrm{APE}_i + \mathrm{AEE}_i}. \quad (4.13)$$

The results show that the wave energy is essentially independent of the amplitude of $\Delta T$, with that for warming being slightly greater than that for cooling. The results for the isothermal case are consistent with the linear results (Bannon 1995a) that a fraction $\kappa = R/C_p = 28\%$ of the available energy generated by the heating is lost to the waves. This fraction is not a fundamental property of the fluid, however. Figure 3 shows that the fraction decreases with increasing stability of the base state. This decrease reflects the fact that the APE is inversely proportional to the static stability [see (4.9)]. For $\Delta T = 1$ K, $A_{\mathrm{waves}} = 34.01\%$, 28.60%, and 11.85% for $\Gamma = -2.8$, 0, and 6.5 K km$^{-1}$, respectively. These fractions are insensitive to changes in the vertical extent (i.e., $a$) or shape (i.e., top hat, parabolic, or sinusoidal) of the heating.

Though the linear theory accurately predicts $A_{\mathrm{waves}}$, its prediction for the partitioning of the energy between the heated layer and the region aloft [see Bannon (1995a), section 5 and Fig. 3] is qualitatively incorrect. It agrees with the nonlinear result only in the limit $a/H_S \to 0$ of a thin layer of heating. We attribute this behavior to the fact that the present results are obtained accurately for a Lagrangian integration, while the linear analysis neglects the displacement of the fluid parcels in the energy calculation.

## 5. Comparison with soundproof solutions

### a. Anelastic solutions

The anelastic continuity equation takes the form

$$\frac{D\rho_0}{Dt} + \rho_0 \nabla \cdot \mathbf{u} = 0, \quad (5.1)$$

where $D/Dt$ is the material derivative. Then the analog of (2.7) is that $\rho_0 dz = \text{const}$. Thus, $z_f = z_i = z_0$ and $\zeta = 0$. There is no expansion or contraction of the gas, and individual air parcels remain fixed in space. This behavior suggests an instantaneous adjustment. It is important to note that (5.1) does not imply the conservation of mass. Rather, it will be shown that the generation of density perturbations in the anelastic adjustment problem implies a redistribution of mass.

The final state variables differ from those of the base state since the heating changes the entropy of the gas. Integration of the anelastic heat equation

$$\frac{D\theta}{Dt} = \frac{\theta_0 Q}{\rho_0 C_p T_0} \quad (5.2)$$

yields the anelastic solution for the potential temperature field

$$\theta_f(z_0) = \theta_i(z_0) = \theta_0\left(1 + \frac{\delta T}{\gamma T_0}\right), \qquad (5.3)$$

with $\delta T$ defined by (2.6). The pressure field may be found from the anelastic hydrostatic equation:

$$\frac{d}{dz}\left(\frac{p_f'}{\rho_0}\right) = \frac{g\theta_f'}{\theta_0}, \qquad (5.4)$$

where primes denote departures from the base state (e.g., $\theta_f' = \theta_f - \theta_0$). Multiplying (5.4) by $\rho_0$ and taking the derivative with respect to height yields (4.4) of Bannon (1995b) and the solution for the pressure field is

$$p_f'(z) = \kappa\rho_0(z)gQ_{00}\int_{-b}^{z}\frac{q(z')}{p_0(z')}\,dz'. \qquad (5.5)$$

Thus, the nonlinear anelastic problem is identical to the linear problem. This finding reflects the fact that the anelastic theories assume that the variations of the state variables are small compared with the base state.

Though the results (5.3) and (5.5) hold for either the Dutton and Fichtl (1969) and the Lipps and Hemler (1982, 1985) equations, the final solutions for the density and temperature fields differ for the two theories. The density field is given by

$$\frac{\rho_f'}{\rho_0} = \frac{p_f'}{\rho_0 g H_\rho} - \frac{\theta_f'}{\theta_0} \qquad (5.6)$$

for the Dutton–Fichtl theory, where $H_\rho^{-1} = -d\ln\rho_0/dz$ is the density scale height, and

$$\frac{\rho_f'}{\rho_0} = \frac{p_f'}{p_0} - \frac{\theta_f'}{\theta_0} \qquad (5.7)$$

for the Lipps–Hemler theory. For either theory the temperature field may then be found using

$$\frac{T_f'}{T_0} = \frac{p_f'}{p_0} - \frac{\rho_f'}{\rho_0}. \qquad (5.8)$$

Application to Lamb's problem allows us to discriminate between the approximations (5.6) and (5.7). Note that these approximations are identical for an isothermal atmosphere and thus the two theories yield the same result in that case (Bannon 1995b).

Figure 4 compares the predictions of the two theories with the compressible solution for the case of a top hat heating profile in a standard atmosphere with $\Gamma = 6.5$ K km$^{-1}$. Use of the top hat heating profile was chosen for continuity with the linear analysis of Bannon (1995a) for an isothermal atmosphere. The same qualitative findings hold for a different heating profile but without the discontinuities in the density and thermal fields. The comparison is made for the case of a small amplitude heating since, as noted above, the anelastic solutions fail to capture the effects of nonlinearity. Specifically, the compressible solution is obtained from the nonlinear numerical solution with $\Delta T = 0.1$ K. In order to convert the Lagrangian numerical solution to the linear Eulerian results of the anelastic theories, the perturbation fields are derived using relations of the form

$$p_f'(z_0) = p_f(z_0 + \zeta) - p_0(z_0)$$
$$\approx p_f(z_0) + \frac{dp_0}{dz}\zeta - p_0(z_0). \qquad (5.9)$$

Similar relations are used for all the state variables. The nondimensionalization of the state variables follows (Bannon 1995a)

$$\Delta p = RQ_{00}/C_v, \quad \Delta T = T_*\Delta p/p_*,$$
$$\Delta\rho = \Delta p/RT_*. \qquad (5.10)$$

Figure 4 reveals that the pressure fields predicted by the two theories are the same and agree with the compressible solution in the small amplitude limit. In this discussion agreement means that the numerical results are identical to at least three significant figures. Note that the final $\theta'$ field for the anelastic solution agrees with the initial $\theta'$ field of the compressible solution. This feature also appears in the analytic linear solution for an isothermal atmosphere (Bannon 1995b). This relation is the correct one and is consistent with the fact that the anelastic solution neglects the vertical expansion and displacement of the fluid parcels. For example, the negative potential temperature perturbation above the heating in the compressible case is a result of the parcels being displaced adiabatically upward a distance $\zeta(a)$. Figure 1d depicts this process. Since there is no vertical displacement of the anelastic fluids, their $\theta'$ field, which must conserve the entropy generated by the heating, must agree with the initial $\theta'$ field of the compressible gas that holds before its expansion. This agreement of the anelastic and compressible pressure and potential temperature fields confirms that (5.4) [and hence (5.5)] is the correct relation between the two fields.

As expected the two theories disagree in their predictions of the density and temperature perturbations. The Dutton–Fichtl theory agrees with the compressible solution for these two additional fields. The Lipps–Hemler theory shows significant differences with the compressible solution. For example, (5.7) and (5.8) yield the statement of thermal equivalency

$$\frac{T'}{T_0} = \frac{\theta'}{\theta_0}, \qquad (5.11)$$

for the Lipps–Hemler theory. This relation underestimates the thermal field in the heated layer and neglects the warming aloft due to the thermal advection in the vertical. As a consequence of (5.11), the density field predicted in the Lipps–Hemler theory is also in error.

A final comment regards the conservation of mass. Though the Dutton–Fichtl theory agrees with the compressible solution, mass is not conserved locally. For

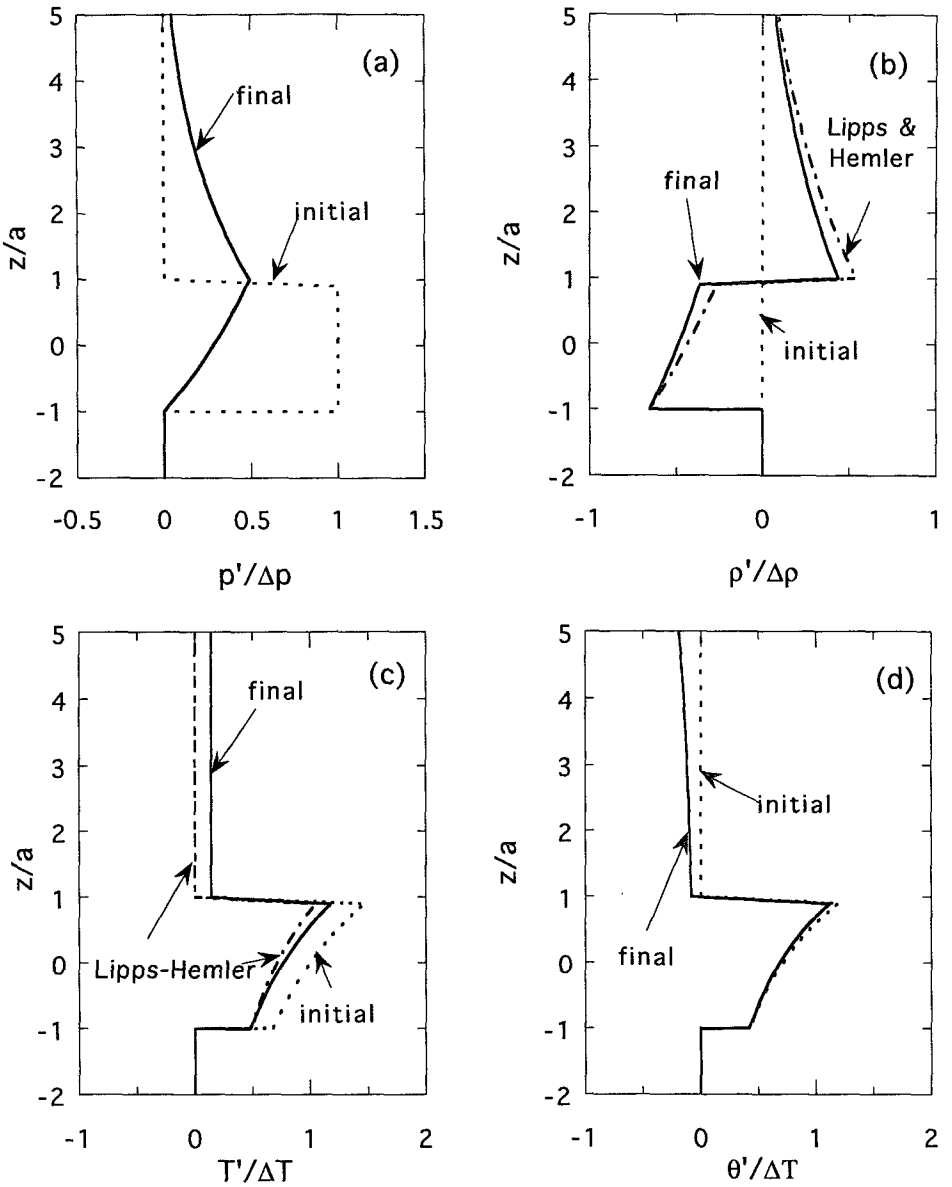


FIG. 4. Vertical profiles of the solutions to Lamb's problem for (a) perturbation pressure $p'$, (b) perturbation density $\rho'$, (c) perturbation temperature $T'$, and (d) perturbation potential temperature $\theta'$. The atmosphere has a standard lapse rate of 6.5 K km$^{-1}$ and the top hat heating profile has a half width $a/H_S = 1/2$. The solid line denotes the compressible solution for the final equilibrium; the dotted line denotes the initial field after the heating. The Dutton–Fichtl solution agrees with the final compressible fields in (a), (b), and (c). The Lipps–Hemler solution is denoted by a dot–dash line. The final pressure perturbations are identical for the three solutions in (a). In (d) the two anelastic solutions predict the same $\theta'$ field, which agrees with the initial $\theta'$ in the compressible case.

example the reduction in density in the heated layer is a result of the expansion in the compressible theory. As we have seen, the anelastic theories predict no such expansion. The density perturbations in the anelastic theory arise from the instantaneous extraction of mass from the heated layer and deposition aloft. Since the Dutton–Fichtl theory predicts the same final density field, mass is conserved globally. Inspection of the $\rho'$ fields in Fig. 4b shows that the perturbation density for the Lipps–Hemler solution is denser than the compressible solution both above and in the heated layer. This structure implies a spurious increase in the mass of the fluid column for the Lipps–Hemler theory.

*b. Pseudo-incompressible theory*

Durran (1989) has advanced an alternative soundproof set of equations. Unlike (5.1) the continuity equation in this theory takes the form

$$\nabla\cdot(\rho_0\theta_0\mathbf{u}) = \frac{\theta_0 Q}{C_p T_0}. \tag{5.12}$$

Use of (2.4) in this equation implies a vertical motion field $w = \zeta(z)\delta(t)$ where the displacement satisfies

$$\frac{d}{dz}(\rho_0\theta_0\zeta) = \frac{\theta_0 Q_{00} q(z)}{C_p T_0}, \tag{5.13}$$

which yields

$$\zeta(z) = \frac{Q_{00}}{\rho_0 C_p \theta_0}\int_{-b}^{z}\frac{\theta_0(z')q(z')}{T_0(z')}\,dz'. \tag{5.14}$$

This result, however, disagrees with the compressible solution (2.17). For example, for a top hat heating profile in an isothermal atmosphere, (5.14) predicts a displacement

$$\zeta(z \geqslant a) = 2\frac{\Delta\zeta}{\kappa}\exp\left[\frac{(1-\kappa)z}{H_S}\right]\sinh\left(\frac{\kappa a}{H_S}\right), \tag{5.15}$$

which increases exponentially with height.

It should also be noted that the pseudo-incompressible theory requires that the thermal equivalency relation (5.11) hold even for nonisothermal conditions. A fundamental scaling assumption of the theory is that $\pi' \ll \pi_0$ but that the other thermodynamic variables may exhibit $O(1)$ variations. Here, the nondimensional quantity $\pi$ is defined by

$$\pi = \frac{T}{\theta} = \left(\frac{p}{p_*}\right)^{R/C_p},$$

so

$$\frac{1+\dfrac{T'}{T_0}}{1+\dfrac{\theta'}{\theta_0}} = 1 + \frac{\pi'}{\pi_0} \approx 1,$$

which implies (5.11). Thus, the pseudo-incompressible theory fails to incorporate the nonlinear form of Lamb's adjustment problem accurately.

*c. Nonhydrostatic, pressure coordinate model*

A nonhydrostatic model that filters acoustic waves but employs a pressure coordinate is due to Miller (1974) and Miller and Pearce (1974). The one-dimensional, nonlinear form of their momentum, continuity, and heat equations are

$$\frac{R}{g}\frac{D}{Dt}\left(\frac{T_0\omega}{p}\right) = -\frac{gp}{RT_0}\frac{\partial\phi'}{\partial p} - g\frac{T'}{T_0}, \tag{5.16}$$

$$\frac{\partial\omega}{\partial p} = 0, \tag{5.17}$$

$$\rho C_p\frac{DT}{Dt} - \omega = Q, \tag{5.18}$$

respectively. Here, $\omega = Dp/Dt$, $D/Dt = \partial/\partial t + \omega\partial/\partial p$ is the material derivative, and $T'$ and $\phi'$ are the perturbation temperature and geopotential, respectively. The base state is a function of pressure, for example, $T_0 = T_0(p)$. Similarly, $Q = Q_{00}q(p)\delta(t)$.

The continuity equation (5.17) implies that $\omega$ is a constant independent of pressure. Application of the lower boundary condition that $\omega = 0$ at $p$ ($z = -b$) implies that $\omega$ vanishes everywhere. This condition is justified as follows. Since the adjustment is instantaneous and both the base state and the final state are hydrostatic, the surface pressure is fixed by the conservation of mass in the fluid column and requires $Dp/Dt = 0$ at the lower boundary. Thus, $\omega = Dp/Dt = 0$ everywhere.

The heat equation (5.18) with $\omega = 0$ may be written as

$$\frac{\partial \ln T}{\partial t} = \frac{RQ}{C_p p}, \tag{5.19}$$

using the ideal gas law. Integration across the delta function in time yields

$$\frac{T}{T_0} = \exp\left[\frac{RQ_{00}q(p)}{C_p p}\right]. \tag{5.20}$$

The vertical momentum equation with $\omega = 0$ reduces to

$$\frac{\partial\phi'}{\partial \ln p} = -RT'. \tag{5.21}$$

Integration of (5.21) upward from the surface $z = -b$ yields an equation for the vertical displacement, $\zeta = \phi'/g$,

$$\zeta(z) = \int_{-b}^{z}\frac{T'}{T_0}\,dz. \tag{5.22}$$

Note that the vertical displacement $\phi'/g$ is the displacement of a pressure surface. But since pressure is conserved following an air parcel ($\omega = Dp/Dt = 0$ everywhere), this displacement also corresponds to the displacement of a fluid parcel. The conservation of pressure also justifies the specification of the heating $Q$ in terms of pressure, $Q = Q_{00}q(p)\delta(t)$.

Substitution of (5.20) into (5.22) yields a nonlinear expression for the displacement that is inconsistent with (2.17), but the small amplitude version agrees

with the correct result (2.20). However, linearization of (5.20) yields the result

$$\frac{T'}{T_0} = \frac{Q_{00}q(z)}{\rho_0 C_p T_0}. \tag{5.23}$$

This result implies that $T'/T_0$ of the present model is identical to the $\theta'/\theta_0$ field of the anelastic problem [cf. (5.23) with (5.3)]. Since (5.11) also holds for the Miller (1974) model, the nonhydrostatic pressure coordinate model suffers from the same shortcoming as the theory of Lipps and Hemler and is inaccurate for a nonisothermal base-state atmosphere. The extension of the Miller and Pearce model by White (1989) does not alter this conclusion.

## 6. Conclusions

The nonlinear solution for the final equilibrium state in Lamb's hydrostatic adjustment problem has been presented. The solution indicates that the linear solution is a good approximation of the adjustment for typical atmospheric situations. The major shortcoming of the linear solution is its prediction of the partitioning of the available energy between the heated layer and the region aloft. The exact nonlinear theory of section 4 indicates that the changes in the available elastic energy initially generated by the heating is completely dispersed by the acoustic modes during the adjustment process. The fraction of available wave energy is independent of the amplitude of the heating but decreases with decreasing base-state static stability. For typical tropospheric values of the stability, this fraction is 12%. In contrast (section 3) the fraction of the heat exchange lost to acoustic modes is small (0.06% for a mean temperature change of 1 K) and increases linearly with the heating but is independent of the static stability. Application of the theory of Andrews (1981) has enabled a direct comparison of the linear and nonlinear energetics.

It is noted that, in general, the fraction of energy lost to the acoustic modes is a function of the time-dependence of the heating. For example, linear theory indicates that heating at a frequency below the acoustic cutoff frequency will not excite any acoustic modes. The present results hold rigorously only for the instantaneous heating (2.4). In linear theory the solution to a delta-function forcing contains information on the nature of the response at all frequencies since the general solution may be found by convolution.

The present results have an interesting application. Typically, the troposphere cools steadily and relatively uniformly at a rate of 1–2 K day$^{-1}$ due to radiative processes. This steady cooling implies a steady contraction of the troposphere of about 20–40 m day$^{-1}$. This contraction must be compensated in the mean by episodic expansion associated with diurnal warming and localized latent heat release.

Four versions of the soundproof equations of motion have been examined to assess their ability to incorporate the acoustic adjustment process. These theories include those of Dutton and Fichtl (1969), Miller and Pearce (1974), Lipps and Hemler (1982), and Durran (1989). None of these theories predict the finite amplitude solutions accurately. Of the four, only the theory of Dutton and Fichtl (1969) provides a solution consistent with the small-amplitude compressible theory for a nonisothermal atmosphere. The implication of this finding on anelastic theory is explored in Bannon (1996). A different test of the anelastic equations appears in Nance and Durran (1994).

*Acknowledgments.* I thank Sukyoung Lee for helpful discussion and an anonymous reviewer for constructive criticism. Partial financial support was provided by the National Science Foundation (NSF) under NSF Grant ATM-9521299.

REFERENCES

Andrews, D. G., 1981: A note on potential energy density in a stratified compressible fluid. *J. Fluid Mech.*, **107,** 227–236.

Bannon, P. R., 1995a: Hydrostatic adjustment: Lamb's problem. *J. Atmos. Sci.*, **52,** 1743–1752.

——, 1995b: Potential vorticity conservation, hydrostatic adjustment and the anelastic equations. *J. Atmos. Sci.*, **52,** 2302–2312.

——, 1996: On the anelastic approximation for a compressible atmosphere. *J. Atmos. Sci.*, **53,** 3618–3628.

Doolittle, J. S., and F. J. Hale, 1983: *Thermodynamics for Engineers.* Wiley, 588 pp.

Durran, D. R., 1989: Improving the anelastic approximation. *J. Atmos. Sci.*, **46,** 1453–1461.

Dutton, J. A., and G. H. Fichtl, 1969: Approximate equations of motion for gases and liquids. *J. Atmos. Sci.*, **26,** 241–254.

Glendening, J. W., 1993: Nonlinear displacement of the geostrophic velocity jet created by mass imbalance. *J. Atmos. Sci.*, **50,** 1617–1628.

Lipps, F. B., and R. S. Hemler, 1982: A scale analysis of deep moist convection and some related numerical calculations. *J. Atmos. Sci.*, **39,** 2192–2210.

——, and ——, 1985: Another look at the scale analysis for deep moist convection. *J. Atmos. Sci.*, **42,** 1960–1964.

Mihaljan, J. M., 1963: The exact solution of the Rossby adjustment problem. *Tellus,* **15,** 150–154.

Miller, M. J., 1974: On the use of pressure as vertical coordinate in modeling convection. *Quart. J. Roy. Meteor. Soc.*, **100,** 155–162.

——, and R. P. Pearce, 1974: A three-dimensional primitive equation model of cumulonimbus convection. *Quart. J. Roy. Meteor. Soc.*, **100,** 133–154.

Nance, L. B., and D. R. Durran, 1994: A comparison of the accuracy of three anelastic systems and the pseudo-incompressible system. *J. Atmos. Sci.*, **51,** 3549–3565.

Nicholls, M. E., and R. A. Pielke, 1994: Thermal compression waves. Part I: Total-energy transfer. *Quart J. Roy. Meteor. Soc.*, **120,** 305–332.

White, A. A., 1989: An extended version of a nonhydrostatic, pressure coordinate model. *Quart J. Roy. Meteor. Soc.*, **115,** 1243–1251.